(33) Llorente, M. A.; Mark, J. E. *J. Polym. Sci., Polym. Phys. Ed.* **1980**, *18*, 181.
(34) Andrady, A. L.; Llorente, M. A.; Mark, J. E. *J. Chem. Phys.* **1980**, *73*, 1439.
(35) Andrady, A. L.; Llorente, M. A.; Mark, J. E. *J. Chem. Phys.* **1980**, *72*, 2282.
(36) Mark, J. E.; Llorente, M. A. *J. Am. Chem. Soc.* **1980**, *102*, 632.
(37) Llorente, M. A.; Andrady, A. L.; Mark, J. E. *J. Polym. Sci., Polym. Phys. Ed.* **1981**, *19*, 621.
(38) Pan, S. J.; Mark, J. E. *Polym. Bull. (Berlin)* **1982**, *7*, 553.
(39) Zhang, Z.-M.; Mark, J. E. *J. Polym. Sci., Polym. Phys. Ed.* **1982**, *20*, 473.
(40) Bevington, P. B. *Data and Error Analysis for the Physical Sciences*; McGraw-Hill: New York, 1968; p 140.
(41) Flory, P. J.; Shih, H. *Macromolecules* **1972**, *5*, 761.
(42) Kuwahara, N.; Okazawa, T.; Kaneko, M. *J. Polym. Sci., Part C* **1968**, *23*, 543.
(43) Delmas, G.; Patterson, D.; Bhattacharyya, S. N. *J. Phys. Chem.* **1964**, *68*, 1468.
(44) Morimoto, S. *Makromol. Chem.* **1970**, *133*, 197.
(45) Speir, J. L. *Adv. Organomet. Chem.* **1979**, *17*, 407.
(46) Gustavson, W. A.; Epstein, P. S.; Curtis, M. D. *J. Organomet. Chem.* **1982**, *238*, 87.
(47) Leung, Y. K.; Eichinger, B. E. *J. Chem. Phys.* **1984**, *80*, 3885.
(48) Ilvasky, M.; Dusek, K. *Polymer* **1983**, *24*, 981.
(49) Candau, F.; Strazielle, C.; Benoit, H. *Eur. Polym. J.* **1976**, *12*, 95.
(50) Flory, P. J.; Hoeve, L. A. J.; Ciferri, A. *J. Polym. Sci.* **1959**, *34*, 337.
(51) Flory, P. J.; Hoeve, C. A. J.; Ciferri, A. *J. Polym. Sci.* **1960**, *45*, 235.
(52) Flory, P. J. *Macromolecules* **1979**, *12*, 119.
(53) Flory, P. J. *Statistical Mechanics of Chain Molecules*; Interscience: New York, 1969.
(54) Flory, P. J. *J. Chem. Phys.* **1977**, *66*, 5720.
(55) Flory, P. J. *Proc. R. Soc. London, A* **1976**, *351*, 351.
(56) Allen, G.; Holmes, P. A.; Walsh, D. J. *Faraday Discuss. Chem. Soc.* **1974**, *57*, 19.
(57) Allen, G.; Egerton, P. L.; Walsh, D. J. *Polymer* **1976**, *17*, 65.
(58) Flory, P. J.; Tatara, Y. *J. Polym. Sci., Polym. Phys. Ed.* **1975**, *13*, 683.
(59) Flory, P. J.; Erman, B. *Macromolecules* **1982**, *15*, 800.
(60) Ball, R. C.; Edwards, S. F. *Macromolecules* **1980**, *13*, 748.
(61) Ball, R. C., private communication.
(62) *Selected Values of Physical and Thermodynamic Properties of Hydrocarbons and Related Compounds*; Carnegie: Pittsburgh, PA, 1953; A. P. I. Project 44: (a) Table 5d; (b) Table 23a.

# Integral Equation Theory of Polymer Melts: Intramolecular Structure, Local Order, and the Correlation Hole†

**Kenneth S. Schweizer* and John G. Curro**

*Sandia National Laboratories, Albuquerque, New Mexico 87185.*
*Received November 20, 1987; Revised Manuscript Received April 4, 1988*

ABSTRACT: Our previously proposed microscopic, off-lattice theory of the equilibrium structure of dense polymer liquids is further developed in regard to the treatment of intramolecular polymer structure. A general scheme for self-consistently calculating the intramolecular and intermolecular pair correlations is outlined, along with the implementation of the integral equation theory for arbitrary ideal polymer models. A simple mathematical procedure for rigorously removing all unphysical intramolecular nonbonded monomer overlap is formulated in general and implemented for the freely jointed chain. The influence of the constant bond length and nonoverlapping constraints on the single-chain structure factor is studied numerically and discussed in the context of recent small-angle neutron-scattering experiments. An extensive series of model calculations of the intermolecular radial distribution function are performed for athermal polymer melts composed of Gaussian chains, Gaussian rings, and ideal and nonoverlapping freely jointed chains. The detailed dependence of both the local, short-range order and the correlation hole on degree of polymerization, density, and intramolecular flexibility is established, along with the limiting behavior for infinite molecular weight.

## I. Introduction

The first tractable, microscopic, statistical mechanical theory for the equilibrium structure of dense one-component polymer melts in continuous space has been recently proposed by the present authors.[1-3] The approach employs an interaction site model of polymer structure and utilizes the integral equation theory of Chandler and Andersen[4,5] developed for small molecule fluids (the so-called "reference interaction site model" or RISM) to compute intermolecular site–site pair correlation functions. The high polymer problem is rendered mathematically tractable by exploiting the near ideality of polymers in the melt[1,2,6-8] and the relative unimportance of chain end effects for long linear macromolecules.[3] The resultant theory is computationally convenient and provides a quantitative description of both long- and short-range order and density fluctuations in dense polymeric liquids. The latter features distinguish our theory from the incompressible random-phase approximation (RPA) approach of deGennes,[6] which addresses only long-range correlations (small wave vector limit) of *labeled* species in the melt. The structural theory can also be employed to calculate thermodynamic properties of the polymer fluid. In principle, our integral equation theory is applicable for arbitrary models of single polymer configurational statistics and short-range intermolecular forces. However, published applications to date[1-3] have focused entirely on Gaussian chains and rings interacting via hard-core repulsions.

The development of a reliable theory of structure and wave vector dependent density fluctuations in polymer melts has many applications to important physical phenomena such as X-ray scattering, neutron scattering, and first-order phase transitions. In addition, the structure and thermodynamics of polymer blends appear to be sensitive to local correlations and compositional fluctuations as recently explicitly demonstrated via computer simulation.[9] A realistic treatment of short-range order in the isotropic liquid requires that some degree of the chemical structure of polymer molecules must be incorporated. In particular, a description of intramolecular structure beyond the

†This work performed at Sandia National Laboratories, supported by the U.S. Department of Energy under Contract DE-AC04-76DP00789.

0024-9297/88/2221-3070$01.50/0 

heavily coarse-grained Gaussian model would seem to be needed. However, the relative importance of specific chemical features (e.g., bond length, bond angle, rotational isomerism, monomer shape) in determining particular observable quantities is a fascinating and largely unexplored question. For example, since low-angle neutron scattering generally probes only small wave vectors, a coarse-grained model of polymer structure may be adequate. Alternatively, wide-angle X-ray scattering is in principle sensitive to the fine details of molecular architecture. However, the simultaneous presence of multiple (chemical) length scales and conformational flexibility in polymer melts tends to wash out sharp *inter*molecular structural correlations even at small monomer–monomer separations and relatively low degrees of polymerization.[10] This fact suggests that including all the fine details of polymeric structure may not be necessary in order to account for observable properties. As a general comment, a theoretical program that incorporates molecular detail in a stepwise fashion, and determines its consequences, would seem to be preferable from the perspective of understanding the influence of various aspects of polymeric structure on bulk liquid thermodynamic properties and correlations.

The present pair of papers represents a first step toward addressing the above issues. After briefly reviewing the RISM theory of polymers in section II, we consider the general problem of intramolecular structure in section III. In particular, we have raised the level of chemical realism a modest amount by studying freely jointed chains in addition to their Gaussian counterparts. However, the ideality assumption still leads to unphysical nonbonded intramolecular monomer overlap, which is clearly unrealistic on very short length scales. To address this problem we develop a simple procedure for treating the intramolecular excluded volume interactions in a melt which completely removes these unphysical overlaps and leads to significant local expansion of the polymer coil. The general problem of a self-consistent treatment of intramolecular and intermolecular correlations is discussed qualitatively. An extensive series of numerical calculations for the intermolecular pair correlation function of hard-core athermal liquids composed of Gaussian chains and rings, and ideal and nonoverlapping freely jointed chains, are presented and discussed in section IV. Special attention is paid to the contact value of the radial distribution function since it plays a central role in the determination of the virial pressure.[11] The detailed dependence of these properties on degree of polymerization, density, and intramolecular structure is established. The paper concludes with a brief summary of our findings. Density fluctuations, the static structure factor, and a comparison of our integral equation results with the predictions of the incompressible RPA and a continuum limit model are the subjects of the following companion paper in this issue.[12]

## II. RISM Integral Equation Theory

The application of matrix integral RISM theory to liquids composed of high polymer chains and rings interacting via hard-core repulsions has been discussed in detail elsewhere.[1-3] In this section we briefly summarize the relevant results.

The generalized Ornstein–Zernike matrix integral equations[4,5] for a one-component fluid composed of polymer molecules containing $N$ sites or chemical subunits interacting via pair-decomposable forces are

$$\mathbf{h}(r) = \int d\vec{r}' \int d\vec{r}'' \, \omega(|\vec{r} - \vec{r}'|)\mathbf{C}(|\vec{r}' - \vec{r}''|)[\omega(r'') + \rho\mathbf{h}(r'')] \quad (1)$$

where $\rho$ is the polymer molecule number density and $\mathbf{h}(r)$, $\mathbf{C}(r)$, and $\omega(r)$ are $N \times N$ matrices with elements $h_{\alpha\gamma}(r)$, $C_{\alpha\gamma}(r)$, and $\omega_{\alpha\gamma}(r)$, respectively. The function $h_{\alpha\gamma}(r) \equiv g_{\alpha\gamma}(r) - 1$ is the correlated part of the intermolecular site–site radial distribution function, $C_{\alpha\gamma}(r)$ is the corresponding direct correlation function between sites $\alpha$ and $\gamma$ on different polymer molecules, and $\omega_{\alpha\gamma}(r)$ is the normalized *intra*molecular probability distribution function, which for the present section is assumed known. In principle, $\mathbf{h}(r)$ is a nonlinear functional of $\omega(r)$, and vice versa, requiring that the two sets of correlation functions be determined self-consistently.[5] The physical idea behind eq 1 is that the intermolecular pair correlations are propagated in a sequential fashion by "chains" of intramolecular and direct pair correlations. The direct correlation function plays a central role in modern liquid-state theory since it provides the means by which the nearly singular repulsive interactions in dense media can be theoretically handled in a nonperturbative manner. It can be interpreted as an effective or renormalized pair potential in the liquid that is a functional of both intramolecular structure and thermodynamic state.[5]

The set of coupled, nonlinear integral equations in eq 1 is closed by introducing a relationship (which is the approximation) between $\mathbf{C}(r)$, $\mathbf{h}(r)$, and the site–site interaction potentials. There are a variety of different schemes for accomplishing the closure depending on the type of chemical system of interest.[5,13-15] For many nonpolar and moderately polar liquids interacting via a relatively short-range site–site potential, the packing forces dominate the structure.[5] In this case, a hard-core interaction is a good approximation, and the corresponding closure relations are

$$h_{\alpha\gamma}(r) = -1; \qquad r < \sigma_{\alpha\gamma} \quad (2a)$$

$$C_{\alpha\gamma}(r) = 0; \qquad r > \sigma_{\alpha\gamma} \quad (2b)$$

where $\sigma_{\alpha\gamma}$ is the distance of closest approach between sites $\alpha$ and $\gamma$. Equation 2a is an exact statement, while eq 2b is the fundamental approximation. Equations 1 and 2 define the RISM theory of hard-core molecular fluids.[4,5] The effects of intramolecular constraints and correlations on the intermolecular packing are explicitly taken into account by the RISM theory in an average fashion.[1,2,5]

For high polymers a direct numerical solution of the $N(N + 1)/4$ coupled, nonlinear integral equations is intractable. We therefore have considered polymer rings and developed an approximation scheme for linear chains composed of identical monomers (sites).

**A. Ring Polymers.** As an obvious consequence of the topological symmetry of a ring, all intermolecular correlation functions in eq 1 are equivalent on average

$$h_{\alpha\gamma}(r) = h(r) = g(r) - 1$$

$$C_{\alpha\gamma}(r) = C(r) \quad (3)$$

This results in an enormous simplification since the matrix integral equations rigorously reduce[16] to a single equation given by[1,2]

$$h(r) = \int d\vec{r}' \int d\vec{r}'' \, \omega(|\vec{r} - \vec{r}'|)C(|\vec{r}' - \vec{r}''|)[\omega(r'') + \rho_m h(r'')] \quad (4)$$

where $\rho_m \equiv N\rho$ is the monomer or site density and $\omega(r)$ is the single-ring polymer structure factor

$$\omega(r) \equiv \sum_{\alpha=1}^{N} \omega_{\alpha\gamma}(r) \quad (5)$$

The closure relations for eq 4 are the site-index inde-

pendent versions of eq 2. Generalization of the integral equation theory to polymers composed of a small number of chemically distinct sites or monomers is straightforward.

**B. Linear Chains.** A computationally tractable approach to the linear chain problem has been recently developed[3] by us based on the simple idea that chain end effects are expected to be small for large $N$. The detailed development is discussed elsewhere,[3] but the idea is to take the linear chain structure into account in an average fashion neglecting the *explicit* chain end effects, i.e., $h_{\alpha\gamma}(r) = h(r)$ and $C_{\alpha\gamma}(r) = C(r)$ for all $\alpha$ and $\gamma$. In the context of our integral equation theory such an approximation can be formulated in an optimum manner, which minimizes errors in *collective* quantities such as $\sum_{\alpha,\gamma} h_{\alpha\gamma}(r)$. The result is a single integral equation identical in form with the ring polymer case (eq 4) *but* where $\omega(r)$ is the single-*chain* structure factor

$$\omega(r) \equiv N^{-1} \sum_{\alpha,\gamma=1}^{N} \omega_{\alpha\gamma}(r) \tag{6}$$

Systematic and mathematically tractable procedures to calculate corrections to the chain-averaged theory have been presented.[3] However, for the collective or averaged radial distribution function defined as

$$g(r) \equiv N^{-2} \sum_{\alpha,\gamma=1}^{N} g_{\alpha\gamma}(r) \tag{7}$$

a large degree of cancellation of errors is expected. This follows from the fact that the leading order correction to our approximation scheme[3] for $g(r)$ vanishes for *all* $N$. Many properties of experimental interest, such as the equation-of-state in the high polymer limit[11] and the static structure factor of neat melts, depend only on collective or "doubly-summed" correlation functions. Equations 2, 4, and 5 (or 6) can be solved numerically by utilizing standard procedures discussed elsewhere.[2,3,5,17]

## III. Intramolecular Structure

There are two distinct aspects related to the treatment of the intramolecular structure of polymers in the melt. The first pertains to the level of chemical detail and constitutes the adoption of a mathematical model that specifies the *short-range* interactions between nearby monomers and associated bonding constraints. Typically, the model can vary widely in complexity all the way from the highly simplified Gaussian model up to a chemically realistic rotational isomeric state description.[18] The second fundamental aspect involves the treatment of the nonbonded intramolecular excluded volume interactions and their self-consistent modification by the presence of other polymer molecules in the dense melt. Both these issues must be addressed in order to implement the RISM integral equation theory.

**A. Ideal Limit.** In our previous work[1-3] the simplest possible approaches to the above two issues were adopted: ideal Gaussian chains and rings were studied. The ideality principle of Flory[7] states that for flexible polymers in the melt the intramolecular configuration is determined entirely by short-range effects; i.e., the strong intra- and intermolecular excluded volume interactions effectively cancel. A litany of both neutron-scattering experiments on labeled chains[8] and computer simulations[10,19] have documented the fundamental correctness of Flory's ideas, including the noteworthy fact that the configurations of monomer sequences much shorter (as small as 10 Å) than the global chain dimension obey ideal statistics unperturbed by intramolecular or intermolecular excluded volume interactions.[20-22] There are, of course, systems and situations for which the ideality theorem either incurs quantitative errors or may break down entirely. We will discuss these subsequently, but first we summarize various "ideal" models that can be studied with our integral equation theory and their corresponding intramolecular structure factors.

For Gaussian ring polymers, with statistical segment length $d$, the intramolecular structure factor is[1,2,23]

$$\hat{\omega}(k) = 1 + 2N^{-1} \sum_{t=1}^{N-1} (N - t) \exp[-k^2 d^2 t(N - t)/6N] \tag{8}$$

and the sum must be computed numerically. For Gaussian and freely jointed chains the structure factor can be analytically[24] calculated with the result

$$\hat{\omega}(k) = (1 - f)^{-2}[1 - f^2 - 2N^{-1}f + 2N^{-1}f^{N+1}] \tag{9}$$

where

$$f = \exp(-k^2 d^2/6) \tag{10}$$

for the Gaussian chain and

$$f = \sin(kl_0)/kl_0 \tag{11}$$

for a freely jointed chain with a fixed bond length $l_0$. Semiflexible wormlike chains can also be treated approximately.[25] Finally, at the expense of significantly more numerical effort, the intramolecular structure factor of rotational isomeric state chains can in principle be calculated by either Monte Carlo simulation and/or moment expansions.[18,26,27]

The use of ideal forms for $\hat{\omega}(k)$ corresponds to the assumption that intramolecular excluded volume effects can be ignored on *all length scales* and for all liquid densities. Mathematically, this affords a great simplification in the implementation of the RISM theory since $\hat{\omega}(k)$ can be calculated separately without having to determine it self-consistently with the intermolecular correlations. Indeed, a *direct* treatment of the intramolecular excluded volume problem for high polymers which is valid for *all* (not just large) length scales of finite size monomers (not $\delta$-function pseudopotentials[28]) does not exist. Nevertheless, it is clear that intramolecular excluded volume can never be ignored at very small separations since nonbonded monomers on the same chain cannot overlap, and this will always have *local* consequences even if it is negligible on large length scales. This consideration represents the first problem with the literal use of the ideal description. The second fundamental problem with the ideal description is its neglect of a self-consistent link between the intramolecular and intermolecular correlations.[5] Such coupling is inherently nonlinear and can produce a variety of "nonideal" phenomena such as condensed-phase modification of isomeric equilibria,[29,30] locally parallel chain domain structure in high-density/low-temperature liquids composed of stiff polymers,[31] and collapse or expansion of chain dimensions with respect to the unperturbed state.[19,21,22] The formulation of a microscopic statistical mechanical theory to address these issues is qualitatively sketched in the next subsection.

**B. Self-Consistent Treatment of Intramolecular and Intermolecular Correlations. 1. General Formulation.** A general classical statistical mechanical theory of the structure of flexible molecules in condensed phases has been developed by Chandler and Pratt.[32] In our notation, their fundamental result is an expression for the full $N$-body intramolecular distribution function, $\omega[\{\mathbf{R}\}]$, of a tagged molecule immersed in a liquid

$$\omega[\{\mathbf{R}\}] \propto \omega_0[\{\mathbf{R}\}]y[\{\mathbf{R}\}] \tag{12}$$

where $\{\mathbf{R}\}$ denotes a complete set of coordinates necessary

to specify a particular polymer configuration, $\omega_0[\{\mathbf{R}\}]$ is the unperturbed (single molecule) distribution function, and $y[\{\mathbf{R}\}]$ is the cavity distribution function or influence functional for a polymer in the liquid.[32] The latter quantity describes the condensed-phase modification of the intramolecular potential surface and is the Boltzmann factor for the reversible work associated with altering configurations of the polymers, i.e.

$$\ln y[\{\mathbf{R}\}] = -\beta\Delta\mu[\{\mathbf{R}\}] \tag{13}$$

where $\Delta\mu[\{\mathbf{R}\}]$ is the solvent (i.e., surrounding polymer molecules) induced part of the potential of mean force. The unperturbed distribution function can also be expressed (within classical mechanics) as a Boltzmann factor of a "bare" potential energy which can be separated into its short-range, "ideal" part, $U_0$, and a part describing the long-range intramolecular excluded volume interactions, $U_E$, which is generally taken to be pair decomposable. Therefore, the full $N$-body distribution function can be written as an exponential of a potential of a mean force: $\omega(\mathbf{R}) \propto \exp(-\beta W)$ where

$$W[\{\mathbf{R}\}] \equiv U_0 + U_E + \Delta\mu \tag{14}$$

If one has an explicit expression for the condensed-phase component, $\Delta\mu$, then *in principle* the effective intramolecular configurational statistics problem defined by eq 14 can be solved, and the corresponding pair or two-body functions $\{\omega_{\alpha\gamma}(r)\}$ required by the RISM theory can be obtained. However, in practice $\Delta\mu$ is exceedingly complex and not even pair decomposable,[33] reflecting the fact that the potential of mean force associated with one pair of sites depends on the configuration of many other sites. This physical feature has been discussed in detail by Chandler et al.[33,34] within the context of the quantum solvated electron problem and the path-integral formulation of quantum mechanics.[35] As emphasized by Chandler, their analysis is quite general and is applicable to real classical, flexible polymeric systems. A self-consistent mean field scheme has been developed to address this problem.[33] The basic result is that the solvent-induced interactions are approximated as pair decomposable but must be determined self-consistently since they are a functional of *both* the intramolecular and intermolecular pair correlations functions themselves, $\{\omega_{\alpha\gamma}(r)\}$ and $\{C_{\alpha\gamma}(r)\}$. In the resulting effective intramolecular statistics problem, $U_E$ and $\Delta\mu$ are then both pair decomposable, but a very formidable theoretical problem remains since one has to simultaneously grapple with the short-range (ideal) interactions, intramolecular excluded volume, and a complex solvent-induced potential which itself must be determined self-consistently.

A tractable approximate solution to this problem for real polymers can be formulated based on optimized perturbation theory about a suitably chosen reference system,[25] but this is beyond the scope of the present paper. In this initial work, we shall adopt a much simpler approach guided by simple screening ideas.

**2. Limiting Approximation.** For neat melts the fundamental feature of the pair-decomposable, self-consistently determined solvent-induced potential is that it is strongly attractive at small separations between pairs of polymer sites, thereby favoring a collapsed polymer structure.[34] This qualitative behavior is a consequence of the physical fact that by shrinking the tagged (solute) polymer less solvent free energy change is needed to incorporate it in the dense liquid. This trend is enhanced with increasing solvent density and implies that the intramolecular excluded volume and solvent-induced potential tend to cancel in eq 14, at least in an average or integrated sense.

If the "solvent"-induced screening of the intramolecular excluded volume interactions is almost complete for separations on the order of a monomer size (as is expected for a dense liquid), then a simple *zero-order* scheme for the treatment of intramolecular excluded volume of polymers in the melt can be envisioned: the intramolecular polymer structure can be treated as ideal except for separations less than or equal to the monomer diameter. In other words, for hard-core interactions, nonbonded monomer overlap is rigorously forbidden, but the intramolecular excluded volume has no other consequences. Such an approach would appear to be the simplest nontrivial treatment of nonideality.

**C. Elimination of Intramolecular Overlap.** The simple approximation discussed above corresponds mathematically to adopting the ideal values for the intramolecular distribution functions $\{\omega_{\alpha\gamma}(r)\}$ for separations of nonbonded pairs beyond the contact value and requiring vanishing probability for overlapping configurations. Such a scheme represents a non-Hamiltonian-based approximation and avoids entirely the self-consistency issues and a possible density dependence of the intramolecular structure. Clearly, the molecular weight scaling of the global dimensions of the polymer will still obey ideal random walk statistics, although both long-range and local expansion of the polymer coil over its purely ideal dimensions will occur. In the remainder of this paper we will concentrate on the freely jointed chain, and hence the relevant equations associated with the implementation of the above scheme will be presented only for this case. Analogous results for other ideal polymer statistics models are straightforwardly obtained in principle.

The Fourier transform of the intramolecular probability distribution function between sites $\alpha$ and $\gamma$ of the ideal freely jointed chain is[24]

$$\hat{\omega}_{\alpha\gamma}(k) = [\sin(kl)/kl]^{|\alpha-\gamma|} \tag{15}$$

where $l$ is the fixed bond length. For simplicity, in all our numerical calculations on hard-core chains we chose $l = \sigma$ = hard-core diameter. The treatment of more general ($l \neq \sigma$) "bead–rod" models is straightforward. Our nonoverlapping freely jointed chain model is defined by

$$\omega_{\alpha\gamma}(r) = (2\pi)^{-3}B_{\alpha\gamma}\int \mathrm{d}\vec{k}\, e^{i\vec{k}\cdot\vec{r}}\left[\frac{\sin(k\sigma)}{k\sigma}\right]^{|\alpha-\gamma|}; \quad r \geq \sigma$$
$$\omega_{\alpha\gamma}(r) = 0; \quad r < \sigma \tag{16}$$

for $|\alpha - \gamma| \geq 2$. The factor $B_{\alpha\gamma}$ is defined so $\omega_{\alpha\gamma}(r)$ is normalized to unity, i.e., $\hat{\omega}_{\alpha\gamma}(0) \equiv 1$. Introducing the function

$$\hat{J}_{\alpha\gamma}(K) \equiv \frac{2}{\pi K}\int_0^1 \mathrm{d}R \sin(KR) \times \int_0^\infty \mathrm{d}K' K' \sin(K'R)\left[\frac{\sin(K')}{K'}\right]^{|\alpha-\gamma|} \tag{17}$$

where $R \equiv r/\sigma$ and $K \equiv k\sigma$ are dimensionless variables, one can show that the normalization factors are given by

$$B_{\alpha\gamma} \equiv (1 - \hat{J}_{\alpha\gamma}(0))^{-1} \tag{18}$$

To implement the RISM theory we require the intramolecular structure factor

$$\hat{\omega}(K) = N^{-1}\sum_{\alpha,\gamma=1}^{N}\hat{\omega}_{\alpha\gamma}(K) = 1 + 2N^{-1}\sum_{\tau=1}^{N-1}(N-\tau)\hat{\omega}_\tau(K) \tag{19}$$

where $\tau \equiv |\alpha - \gamma|$. Adding and subtracting the ideal freely

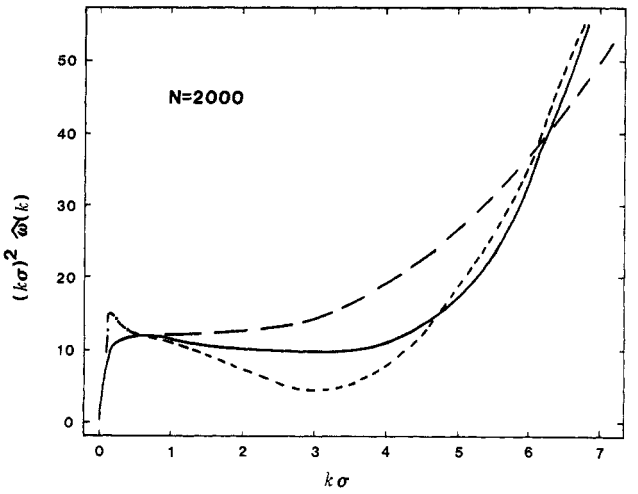


**Figure 1.** Kratky plot of intramolecular structure factor versus dimensionless wave vector for a 2000-unit Gaussian chain (long dash), Gaussian ring (dash-dot), ideal freely jointed chain (solid), and nonoverlapping freely jointed chain (short dash).

jointed structure factor $\hat{\omega}_{id}(K)$ (see eq 9 and 11) and performing a modest amount of algebra yield the result

$$\hat{\omega}(K) = \hat{\omega}_{id}(K) + \frac{2}{N}\sum_{\tau=2}^{N-1}(N-\tau)\left[\hat{\omega}_\tau(K) - \left(\frac{\sin K}{K}\right)^\tau\right] \tag{20}$$

where

$$\hat{\omega}_\tau \equiv B_\tau\left[\left(\frac{\sin K}{K}\right)^\tau - \hat{J}_\tau(K)\right] \tag{21a}$$

$$\hat{J}_\tau(K) \equiv \frac{1}{\pi K}\int_0^\infty dy\, y\left(\frac{\sin y}{y}\right)^\tau\left[\frac{\sin(K-y)}{K-y} - \frac{\sin(K+y)}{K+y}\right] \tag{21b}$$

$$\hat{J}_\tau(0) = \frac{2}{\pi}\int_0^\infty dy\left(\frac{\sin y}{y}\right)^\tau\left[\frac{\sin y}{y} - \cos y\right] \tag{21c}$$

with $B_\tau$ given by eq 18. The sum in eq 20 must be evaluated numerically.

The corresponding radius of gyration of the nonoverlapping freely jointed chain is given by[24]

$$\langle R_g^2\rangle = \frac{1}{2N^2}\sum_{\alpha,\gamma=1}^{N}\langle r_{\alpha\gamma}^2\rangle = \frac{2\pi}{N}\int_0^\infty dr\, r^4\omega(r) \tag{22}$$

where $r_{\alpha\gamma}$ is the distance between sites $\alpha$ and $\gamma$ and $\omega(r)$ is the inverse Fourier transform of eq 20. Straightforward manipulations allow eq 22 to be rewritten as

$$\langle R_g^2\rangle = -\frac{3\sigma^2}{2N}\lim_{K\to 0}\frac{d^2\hat{\omega}(K)}{dK^2} \tag{23}$$

This equation can be evaluated by analytically taking two derivatives of eq 20 and the zero wave vector limit, followed by numerical evaluation of the remaining sum over $\tau$ and one-dimensional integrals.

**D. Numerical Results.** The intramolecular structure factors for a 2000-unit Gaussian ring (eq 8), Gaussian chain (eq 9 and 10), ideal freely jointed chain (eq 9 and 11), and nonoverlapping freely jointed chain (eq 20 and 21) are plotted in Figure 1 in the standard Kratky manner. As expected on physical grounds, the Gaussian chain and ring structure factors are identical except at small wave vectors. For the linear Gaussian chain $k^2\hat{\omega}(k)$ is a *monotonically increasing* function of the wave vector with a near plateau

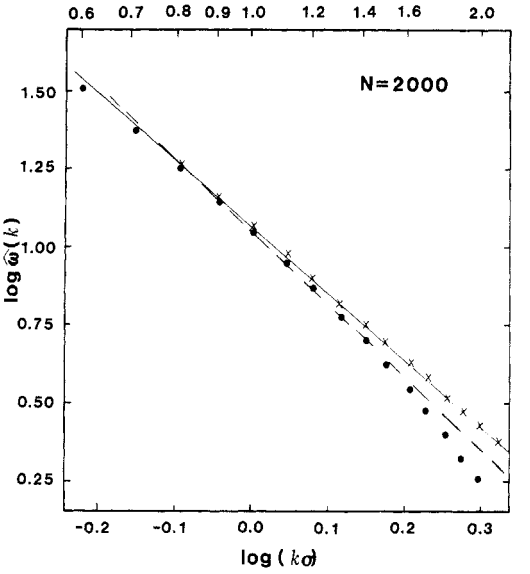


**Figure 2.** log–log plot of the intramolecular structure factor versus dimensionless wave vector for a 2000-unit ideal freely jointed chain (crosses) and nonoverlapping freely jointed chain (solid circles). The lines drawn through the points correspond to linear fits over $k\sigma$ regimes discussed in the text. The top horizontal axis shows the corresponding values of $k\sigma$.

in the intermediate wave vector regime, $R_g^{-1} \ll k < \sigma^{-1}$. The monotonic behavior for the Gaussian chain is of some importance since it implies that any "apparent" power law decay of the structure factor, $\hat{\omega}(k) \sim k^{-\gamma}$, must obey $\gamma \lesssim 2$. For the two freely jointed chain (FJC) cases, the deviations from Gaussian behavior are essentially negligible for $k\sigma \lesssim 0.7$. At large wave vectors, $k\sigma \gtrsim 6$, the FJC behavior is dominated by the constant bond length constraint, and deviations from the ideal case due to the nonoverlapping condition are relatively minor. However, in the regime $0.7 \lesssim k\sigma \lesssim 4$ there are significant differences between the three linear chain models. In particular, both freely jointed chains display a *decrease* in $k^2\hat{\omega}(k)$ in this regime and hence nonmonotonic behavior. The decrease is far more dramatic in the nonoverlapping chain model, and it is in this wave vector regime that the constraint of no intramolecular monomer overlap is most important.

In Figure 2, an expanded log–log plot of the structure factor for $k\sigma \sim 1$ of the two FJC models is presented. We observe that over the entire regime $0.8 \lesssim k\sigma \lesssim 2$ the ideal freely jointed chain displays to a good approximation power law decay of the form $(k\sigma)^{-\gamma}$ with $\gamma \simeq 2.12$. Over the more limited regime $0.8 \lesssim k\sigma \lesssim 1.4$, the nonoverlapping FJC also decays as an approximate power law with an exponent $\gamma \approx 2.33 \pm 0.05$. In general, of course, simple power law behavior is not expected to be valid except over limited wave vector regions. However, experimentalists often characterize their data in such a manner. Our interest in the behavior in the wave vector regime discussed above stems from a variety of neutron-scattering experiments, especially those of Bates and Wignall.[36] Many small-angle neutron-scattering measurements on labeled chains are done in the region $k \sim 0.01$–$0.1$ Å$^{-1}$ and can be interpreted in terms of the Gaussian model. We note that typical statistical segment lengths fall in the range $\sigma \sim$ 5–7 Å, and hence the dimensionless quantity $k\sigma \sim$ 0.05–0.7. As seen from Figure 1, in this regime the details of polymer structure are unimportant, with all models displaying Gaussian behavior in agreement with experimental observations. However, recent work at higher wave vectors up to $k \sim 0.2$ Å$^{-1}$ corresponds to system-specific values of $k\sigma$ up to 1.0–1.5. Experimentally, Wignall and

**Table I**
**Expansion Factor $\alpha^2$ for Nonoverlapping Freely Jointed Chains as a Function of the Number of Sites or Monomers, $N$**

| $N$ | $\alpha^2$ | $N$ | $\alpha^2$ |
|---|---|---|---|
| 3 | 1.1250 | 20 | 1.0476 |
| 4 | 1.1480 | 30 | 1.0250 |
| 5 | 1.1463 | 40 | 1.0151 |
| 6 | 1.1377 | 50 | 1.0101 |
| 8 | 1.1174 | 100 | 1.0027 |
| 10 | 1.0999 | 200 | 1.0007 |
| 12 | 1.0859 | 500 | 1.0001 |
| 16 | 1.0644 | | |

Bates[36] have found that Gaussian behavior is sometimes still valid at these higher wave vectors, but for certain materials $\hat{\omega}(k) \sim k^{-\lambda}$, with $\lambda \approx 2.35$ in the higher $k$ regime. We note that our calculations are consistent with such observations and suggest that the observed decay of the single-chain structure factor may be, at least partially, a reflection merely of constant bond lengths and/or intramolecular exclusion of nonbonded monomer overlap.

Another property of considerable importance is the degree of swelling of FJCs introduced by the nonoverlapping condition. The expansion ratio, $\alpha^2 \equiv \langle R_g^2 \rangle / \langle R_g^2 \rangle_{ideal}$, has been computed by using eq 23 as a function of the number of sites, where

$$\langle R_g^2 \rangle_{ideal} = (N + 1)(N - 1)\sigma^2/6N \qquad (24)$$

and represents the mean square radius of gyration of a Markovian, nonreversal random walk in continuous space. Numerical results are summarized in Table I. We note that these results are also indicative of the *local* expansion of finite segments of $N$ sites embedded in a longer polymer coil within the Markov approximation. From the table one sees that the maximum expansion occurs for four sites and monotonically decreases thereafter. Beyond $N = 50$ the enhancement is less than a 1% effect. For chains of 15–20 sites our model predicts an expansion factor of ≈1.05–1.07, which is in excellent agreement with the very high density athermal tetrahedral lattice Monte Carlo calculations of Curro.[19] This agreement provides a degree of indirect support for the utility of our treatment of the effects of intramolecular excluded volume in dense melts.

Ideal descriptions of polymer structure always introduce a finite amount of unphysical nonbonded monomer or site overlap. Therefore, to compute an *average* packing fraction, $\eta_M = \rho V_M$, one needs the average molecular volume, $V_M$, which is given by $V_M = V^{(0)} - \langle V_{ov} \rangle$, where $V^{(0)}$ denotes the molecular volume ignoring site overlap and $\langle V_{ov} \rangle$ is the ensemble-averaged overlap volume. For a general polymer configuration the calculation of $V_{ov}(\mathbf{R})$ and subsequent ensemble average will be very difficult to perform. We have therefore employed a decoupling approximation which reduces the calculation of $V_M$ to knowledge of two-site or pair correlations. Specifically, we make a superposition approximation in which all ≥3-body overlap volumes are computed as if each individual pair was independent. The analysis is straightforward, and we omit the details. For the freely jointed and Gaussian chains and rings of interest here the zero-order volume $V^{(0)} = N\pi\sigma^3/6$, and the resulting effective mean monomer packing fraction is

$$\eta_M = \rho N \frac{\pi}{6} \sigma^3 [1 - \epsilon_N] \qquad (25)$$

where $\epsilon_N$ is the *fractional* overlap volume.

Explicit analytic forms for $\epsilon_N$ are presented in the Appendix. Numerical results employing these forms are listed in Table II for the Gaussian ring and chain and the FJC.

**Table II**
**Fractional Overlap Volume $\epsilon_N$ As Defined in Text for Various Numbers of Sites $N$ and Three Models[a]**

| | $\epsilon_N$ | | |
|---|---|---|---|
| $N$ | GR | GC | FJC |
| 20 | 0.332 | 0.235 | 0.114 |
| 200 | 0.366 | 0.323 | 0.192 |
| 500 | 0.368 | 0.340 | 0.208 |
| 2000 | 0.3691 | 0.354 | 0.222 |
| 4000 | 0.3693 | 0.359 | 0.225 |
| 8000 | 0.3694 | 0.362 | 0.226 |
| 16000 | 0.3695 | 0.364 | |

[a] Gaussian ring (GR), Gaussian chain (GC), and freely jointed chain (FJC).

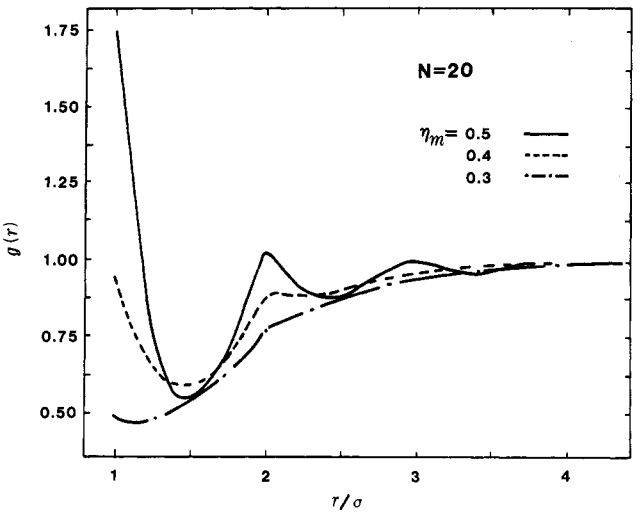


**Figure 3.** Intermolecular radial distribution function plotted versus dimensionless site–site separation for a 20-unit nonoverlapping freely jointed chain and three packing fractions.

As expected, $\epsilon_N$ is an increasing function of $N$ and polymer flexibility. The Gaussian ring $\epsilon_N$ converges considerably faster than the chain, but both appear to approach the same limiting value. Finally, we note that our approximate method for computing $\epsilon_N$ represents an *upper bound* to the true fractional volume overlap, and hence the resulting packing fraction is a *lower bound*. This fact follows immediately since the superposition approximation overestimates the ≥3-body overlaps. Consequently, our calculation of the effective packing fraction will become more accurate as the probability and magnitude of the higher order overlaps decrease.

## IV. Intermolecular Pair Correlations

In this section we present numerical calculations of the intermolecular pair correlation function, $g(r)$, of athermal Gaussian and freely jointed chain models as a function of degree of polymerization, $N$, and the monomer packing fraction, $\eta_M$. Attention is focused primarily on the short-range order. For atomic fluids the appropriate range of liquid packing fractions[14] is $\eta_M \approx 0.32$–$0.5$, and higher values are often of interest for liquids under pressure or as crude models of glasses.[38] The latter point may be especially relevant since neutron-scattering experiments support the idea that the configurational statistics of polymer melts and solid amorphous polymers below their glass transition temperature are equivalent.[39] We have concentrated on the high-density liquid regime, although a few lower density calculations will also be presented.

**A. Local Structure.** Figures 3–5 present results for the $g(r)$ of nonoverlapping FJC at several degrees of polymerization and packing fractions. There are two general comments worth making at the start. First, we have

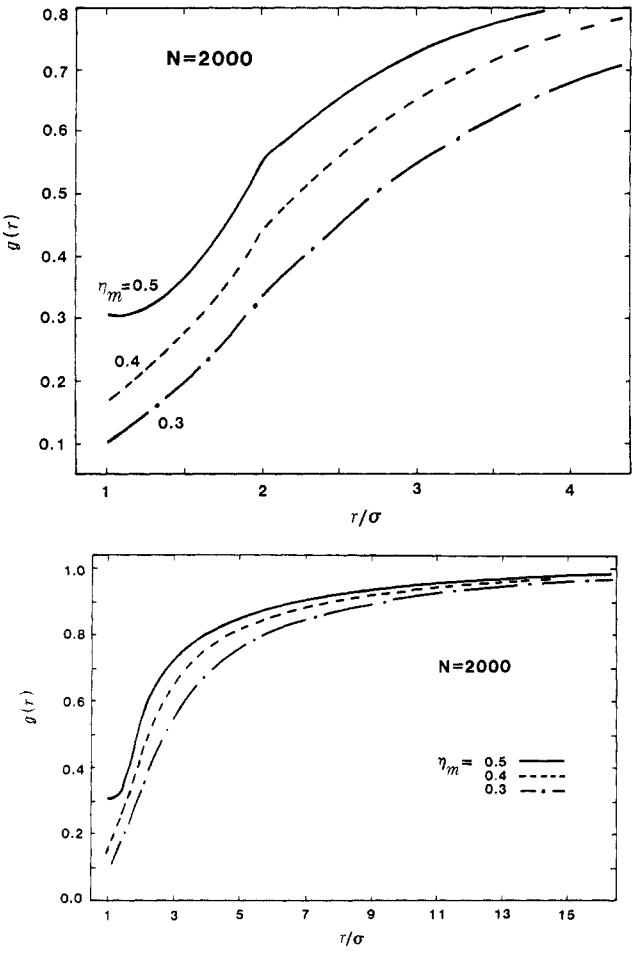


**Figure 4.** (a, Top) Same as Figure 3 except for 2000-unit chain. (b, Bottom) Same as Figure 4a except over an expanded range of separations. The radius of gyration is 18.2574 in dimensionless units.

chosen the interval $1 \leq r/\sigma \leq 4$ as defining the "short-range-order" regime. This is because we have discovered (see the following paper[12]) that for the models under present consideration beyond $r \geq 4\sigma g(r)$ an essentially universal behavior is displayed which is well described by the simple incompressible RPA theory of deGennes.[6] The second comment pertains to the presence of cusplike structures in $g(r)$ at $r/\sigma = 2$. Ladanyi and Chandler[40] have presented a thorough analysis of the occurrence of cusps in hard-core interaction site models and have shown that away from contact cusps are due to intramolecular rigidity and geometric constraints. For a freely jointed chain (ideal or nonoverlapping) the only rigid constraint is the nearest-neighbor bond length, which induces a cusp at $r = 2\sigma$. For completely flexible Gaussian models no cusps occur.

Figure 3 plots $g(r)$ at three packing fractions for a short "alkane-like" $N = 20$ chain. Part of our motivation for studying a small $N$ case is the hope that high-density off-lattice computer simulations of such systems will be performed, thereby providing a direct test of the accuracy of the RISM theory of flexible chain molecules and our approximate treatment of the intramolecular correlations. Progress in modern liquid-state science has been crucially dependent on comparisons between analytic theory and computer simulations of *simple* models.[41] It is our hope that the present work will stimulate an analogous development for polymer liquids. There are several features of Figure 3 worth emphasizing: (1) The contact value, $g(\sigma^+)$, is significantly reduced compared with the disconnected (atomic) limit. In particular, for $N = 1$ the Percus–Yevick results are $g(\sigma^+) = 2.35$, 3.33, and 5.00 for $\eta_M$ = 0.3, 0.4, and 0.5, respectively. Physically, this reduction is a manifestation of self-screening, or the "correlation hole", whereby monomers on different chains are partially excluded from close approach to sites on a tagged polymer coil. Such a phenomenon results from the combined effects of chemical connectivity and the random walk character of flexible coils. (2) The local structure sharpens dramatically with increasing packing fraction leading to multiple peaks at $r/\sigma \approx 2$ and 3. However, the peaks are considerably weaker and more diffuse than in the atomic case because of the large degree of flexibility and multiplicity of length scales present in the chain molecule liquid.

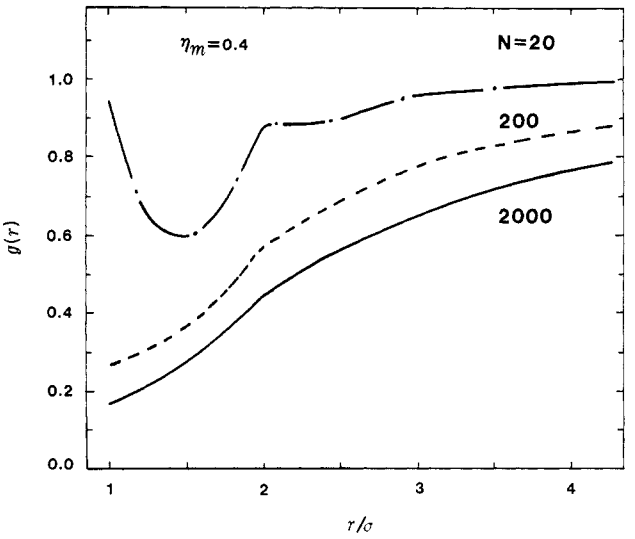


**Figure 5.** Intermolecular radial distribution functions of nonoverlapping freely jointed chains for three values of $N$ at a fixed packing fraction.

Figure 4a presents results for a true high polymer, $N = 2000$, at the same three packing fractions as in Figure 3. Note the apparent lack of structure and the monotonic rise of $g(r)$ toward unity. The magnitude of the contact value is also significantly reduced compared to the $N = 20$ liquid due to the enhanced self-shielding provided by the larger polymer coil. In Figure 4b, $g(r)$ is plotted out to large separations ($R_g = 18.257\sigma$). The functional form of $h(r)$ as it approaches zero does not obey a simple power law. However, if one force fits $h(r) \sim r^{-\lambda}$ over the intermediate length scale regime ($\sigma \ll r < R_g$), then $1 < \lambda < 2$, and $\lambda$ is a decreasing function[12] of $N$ that approaches unity as $N \to \infty$.

Figure 5 presents a comparison of the short-range $g(r)$ at a fixed packing fraction for three values of $N$. Note the enhanced effect of self-shielding with increasing $N$. Qualitatively, increasing $N$ at constant volume produces effects similar to decreasing density at a fixed chain length.

In Figure 6a, packing fraction dependent results for ideal Gaussian chains are presented for $N = 2000$. These correlation functions are essentially devoid of structure and increase monotonically with separation. At the two lower packing fractions, $g(r)$ increases away from contact in an approximately exponential fashion, and the corresponding rate can be interpreted as defining a screening length.[1-3] Figure 6b compares $g(r)$ for several very high molecular weight Gaussian chains at fixed packing fraction plotted as a function of monomer–monomer separation scaled by the radius of gyration, $R_g^2 = N\sigma^2/6$. The contact value is essentially independent of the degree of polymerization. However, the degree of interpenetration increases strongly with $N$ reflecting the more diffuse nature of the random walk coils with increasing radius of gyration.

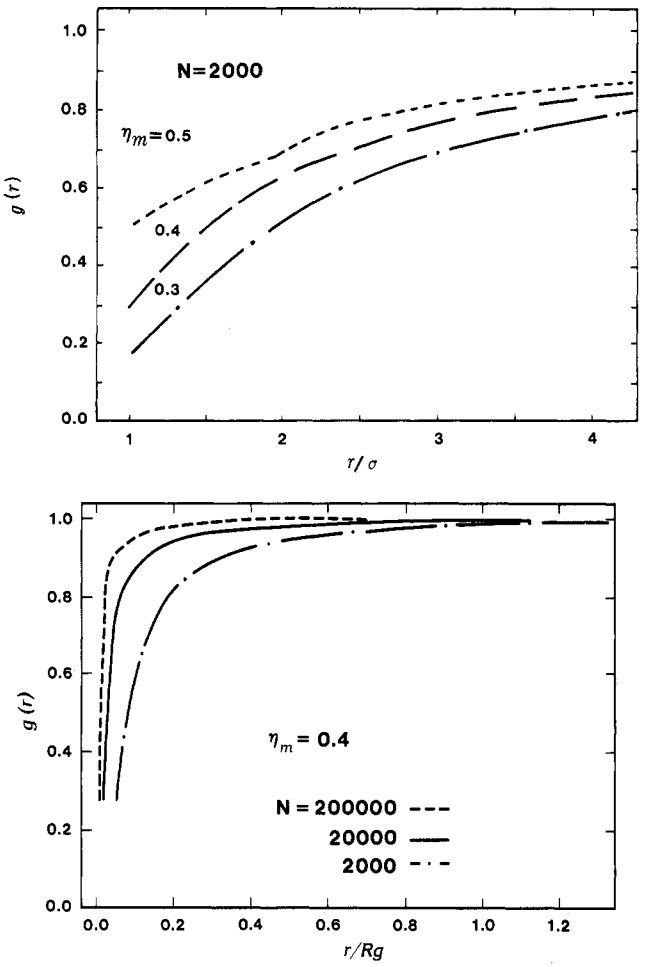


**Figure 6.** (a, Top) Same as Figure 3 but for linear Gaussian chains. (b, Bottom) High molecular weight dependence of the intermolecular radial distribution function of Gaussian chains at a fixed packing fraction plotted as a function of separation scaled by the radius of gyration.

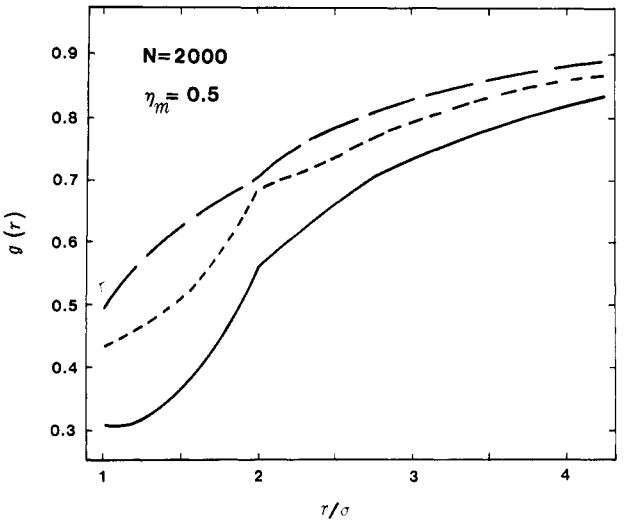


**Figure 7.** Comparison of the intermolecular radial distribution functions of a 2000-unit Gaussian chain (long dash), ideal freely jointed chain (short dash), and nonoverlapping freely jointed chain (solid), at a fixed effective packing fraction.

**Table III**
**Mass Density of Alkane Liquids[42] at Room Temperature and Atmospheric Pressure as a Function of the Number of Carbons, $N^a$**

| $N$ | $\rho$, kg/m$^3$ | $\eta_M$ |
|---|---|---|
| 4 | 605 | 0.461 |
| 6 | 658 | 0.491 |
| 10 | 728 | 0.524 |
| 14 | 761 | 0.538 |
| 18 | 782 | 0.547 |
| ∞ | 840[b] | 0.573 |

[a] $\eta_M$ is the effective packing fraction calculated as described in the text. [b] Obtained by linear (in $N^{-1}$) extrapolation.

Figure 7 compares $g(r)$ for the Gaussian chain, ideal FJC, and nonoverlapping FJC at "constant" packing fraction. Note the significantly different behavior in the $\sigma < r < 2\sigma$ regime and the sharpening of structure as the intramolecular structure "stiffens". The relative absolute values of the different models cannot be taken literally since our computation of the effective packing fraction of ideal chains represents an underestimate (see section III.D). In particular, since we expect the superposition approximation to be less accurate as the ideal polymer becomes more flexible, the ordering of the magnitude $g(r)$ as Gaussian > ideal FJC > nonoverlapping FJC may be entirely due to the uncertainty in the effective $\eta_M$ calculation. This ambiguity is exaggerated at very high densities such as considered in Figure 7 because of the strong dependence of $g(r)$ on the packing fraction.

Figures 3–5 imply a significant $N$ dependence of the local structure at *fixed* packing fraction. For real polymer liquids at atmospheric pressure, however, the density is generally an increasing function of degree of polymerization.[42] Experimental data for hydrocarbon liquids, $(CH_2)_N$, are listed in Table III. Therefore, part of the $N$ dependence predicted by RISM is compensated for in real systems. To crudely address this point, we have imagined our nonoverlapping FJCs represent polymethylene chains and have employed the experimental mass densities in conjunction with a calculation of the molecular volume to determine an $N$-dependent effective packing fraction. Following the analysis of Pratt et al.[29] for butane, we represent the $CH_2$ and $CH_3$ units of polymethylene as spheres of diameter 3.77 Å with a carbon–carbon bond length of 1.52 Å. The volume of an $N$-mer is then

$$V_N = 2v_{END} + (N - 2)v_I \quad (26)$$

where $v_{END}$ = 22.055 Å$^3$ is the volume of a chain end methyl group and $v_I$ = 15.828 Å$^3$ is the average volume contributed by each interior methylene group. The resulting packing fraction is defined as usual as $\tilde{\rho}_N V_N \equiv \eta_M$, where $\tilde{\rho}_N$ is the number of molecules per cubic angstrom. Using eq 26 and the experimental mass densities, we obtain the results listed in the third column of Table III. Theoretical radial distribution functions for freely jointed chains with packing fractions appropriate to $N$ = 20, 200, and 2000 polymethylene chains are presented in Figure 8, where for $N \geq 20$ the effective packing fraction was obtained from a linear fit (in $N^{-1}$) of the results in Table III. Note that the inferred effective packing fractions are very high by simple liquid standards. The resulting $g(r)$ values exhibit significant structure even for $N$ = 2000, and there remains a considerable dependence on degree of polymerization. Finally, we comment that an internally consistent approach would theoretically compute the pressure by employing the RISM theory. This allows a theoretical *determination* of the $N$-dependent packing fraction at *fixed* pressure. Such a program has been carried out and is discussed elsewhere.[11] We find that the $N$ dependence of the resulting $g(r)$ values is substantially weaker than that displayed in Figure 8.

**B. Contact Value.** In this subsection we study the contact value of the intermolecular radial distribution function, $g(\sigma^+)$, as a function of degree of polymerization,

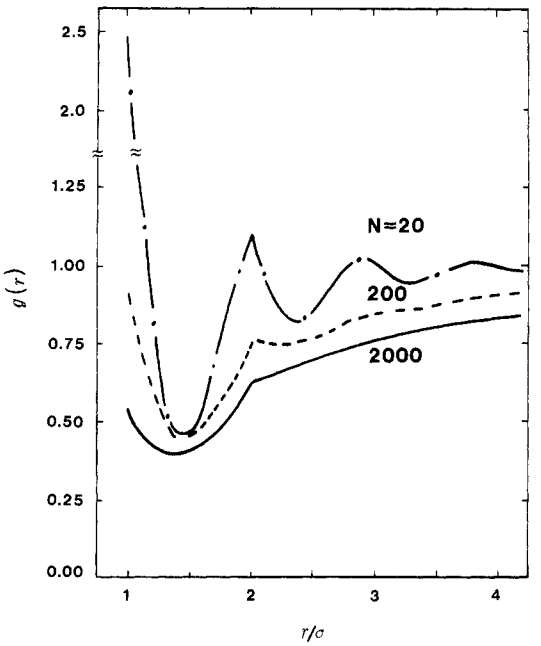


**Figure 8.** Intermolecular radial distribution function of nonoverlapping freely jointed chains at three values of degrees of polymerization. The packing fractions correspond to those typical of real alkane melts (see text) and are given by $\eta_M = 0.549$, 0.571, and 0.573 for $N = 20$, 200, and 2000, respectively. Note the break in the vertical scale.

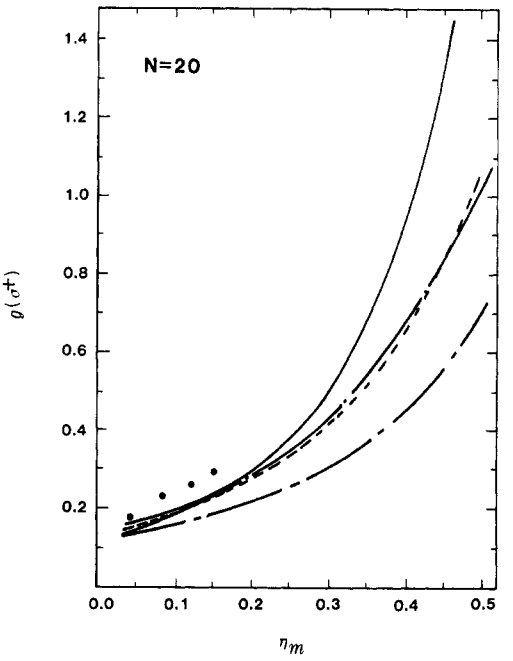


**Figure 9.** Contact value of the intermolecular radial distribution function of 20-unit Gaussian ring (long dash–short dash curve), Gaussian chain (dash-dot), ideal freely jointed chain (short dash), and nonoverlapping freely jointed chain (solid) as a function of packing fraction. The solid circles denote the Monte Carlo results of Curro (see text).

packing fraction, and intramolecular structure. The contact value is the most obvious single measure of short-range order in the liquid and plays a central role in determining the virial pressure of athermal polymer melts.[11] It is the latter point that has motivated our detailed study of the contact value.

Figure 9 displays the results of our numerical calculations over a wide range of packing fractions for four $N = 20$ models: the Gaussian ring, Gaussian chain, and ideal and nonoverlapping freely jointed chains. As an important caveat, we note that our use of an $\hat{\omega}(k)$ in which the global consequences of long-range intramolecular excluded volume effects are screened is not rigorous at very low densities. For $N = 20$, a crude estimate of the semidilute crossover packing fraction[6] is $\eta_M^* \sim N^{-4/5} = 0.091$. For densities lower and possibly somewhat greater than this value one expects extra swelling of the single polymer structure. Turning to a discussion of Figure 9, we first note that the magnitude and density dependence of the contact value at low packing fractions is remarkably insensitive to the details of the *chain* intramolecular structure. This may be somewhat fortuitous due to the approximate nature of our estimate of the packing fraction of ideal chains. Nevertheless, we believe this insensitivity is a real physical effect that arises from the large degree of averaging of intramolecular details that occurs at low density even on short length scales. Note, however, that even at low density the Gaussian ring $g(\sigma^+)$ is significantly less than its linear chain counterpart. This is a result of the more compact nature of the ring and the corresponding enhanced degree of self-screening. As the packing fraction increases into the liquid regime, $g(\sigma^+)$ values of the ideal FJC and Gaussian chains remain very close, and the differences between ring and chain are exaggerated. The former behavior is somewhat surprising and implies that the constant bond length constraint is not very important in an average sense at *fixed* packing fraction. On the other hand, the nonoverlapping FJC exhibits a significantly larger contact value and a stronger density dependence. Presumably, this is a result of the expanded nature of local sequences compared to the ideal case and a concomitant increase in accessible surface area of the polymer chain.

In atomic and small molecule liquid-state theory, the accuracy with which an integral equation approach can predict the contact value is an especially sensitive test of its quantitative reliability. For small, rigid, hard-core molecules (diatomics and triatomics) extensive comparisons between the RISM theory predictions and essentially exact computer simulations have been performed.[43] The detailed conclusions of such comparisons depend to some degree on the specifics of the system. However, the general qualitative trends are that the RISM theory predicts contact values at liquid densities to within roughly ±10–20% of the exact values. Whether such accuracy also applies to moderate and/or long flexible chain and ring molecules is very difficult to judge a priori. Unfortunately, published simulation data at high densities for off-lattice polymer melts are virtually nonexistent due to excessive computational demands. The most appropriate computer results for our purposes are the Monte Carlo simulations of Curro[19] on $N = 15$ and 20 unit freely *rotating* hard-core polymer chains for packing fractions up to $\eta_M = 0.153$. Curro's results for $N = 20$ are the solid circles in Figure 9, and a quantitative comparison with our RISM predictions for nonoverlapping freely jointed chains is made in Table IV. The RISM values of $g(\sigma^+)$ are roughly 20% lower than the Monte Carlo results, and the density dependence are very similar. At higher densities (true liquid) our RISM results appear to be in good agreement with an extrapolation of the Monte Carlo data. A related question is the $N$ dependence of $g(\sigma^+)$. Over the same packing fraction range as in Table IV, Curro's results[19] for $N = 20$ reveal an approximately 10–15% decrease in the contact value relative to the $N = 15$ case, and this is in good agreement with RISM calculations we have performed. A caveat to our comparison with Curro's simulations is that the models were not identical since Curro studied a freely rotating (fixed bond angle) *not* freely jointed chain. In addition, at the relatively low densities considered the

Table IV
**Comparison of the RISM Integral Equation Results for $g(\sigma^+)$ of $N = 20$ Athermal Nonoverlapping Freely Jointed Chain Fluid with Monte Carlo Results of Curro (ref 19) for a Closely Related Model (See Text).**

| $\eta_M$ | Monte Carlo[a] | RISM |
|---|---|---|
| 0.0419 | 0.178 | 0.158 |
| 0.0818 | 0.234 | 0.181 |
| 0.122 | 0.266 | 0.211 |
| 0.153 | 0.292 | 0.238 |

[a] Estimated accuracy is ±5%.

intramolecular excluded volume was probably not fully screened, and hence Curro's chains may be slightly expanded relative to ours. However, both additional simulations of hindered chains by Curro[19] and those of other workers,[44] along with our general finding that $g(\sigma^+)$ is not very sensitive to intramolecular details at low density, suggest these differences have only very modest consequences for $g(\sigma^+)$ (~10–20% effects). Indeed, both differences described above will tend to raise $g(\sigma^+)$ and hence if removed will lower the simulation result, thereby improving agreement with our RISM values.

We interpret the overall agreement discussed above as evidence that the RISM theory is of the same general quantitative accuracy for polymers (at least up to $N = 20$) as it is for hard-core diatomics and triatomics. If true, this is a very significant conclusion, since the availability of a computationally tractable, reliable theory is especially urgent for polymer liquids because brute force off-lattice simulations are so difficult at high densities and realistic molecular weights.

The $N$ dependence of the contact value is plotted in Figure 10 for two packing fractions. Results for the Gaussian ring are not shown in the figure but converge to a limiting value for $N \gtrsim 2000$, which is identical with the limiting Gaussian chain value to within our numerical accuracy. There are several other noteworthy trends in Figure 10: (1) For all three intramolecular structure models $g(\sigma^+)$ decreases strongly with increasing $N$ as a result of the enhanced self-screening characteristic of larger coils. This trend contrasts with the larger degree of global interpretation as $N$ increases and the coils become more diffuse. The $N$ dependences of the Gaussian and ideal freely jointed chains are very similar and correspond roughly to a reduction factor of 2 in $g(\sigma^+)$ on going from $N = 20$ to $N \to \infty$. However, the nonoverlapping freely jointed chain exhibits a much stronger $N$ dependence, with $g(\sigma^+)$ decreasing by roughly a factor of 5–6 over the same range of $N$. This trend is at least partially the result of the fact that a single site of an ideal chain really represents a Kuhn segment and hence a larger number of physical monomers than in the case of the (stiffer) nonoverlapping chain. (2) Convergence to the asymptotic limit is slow. Beyond $N \approx 1000$, $g(\sigma^+)$ approaches its limiting value as a linear function of the inverse degree of polymerization. (3) For relatively short chains ($N \lesssim 100$), the contact value of the nonoverlapping model is larger than that of the corresponding ideal polymer. Such a trend is consistent with excluded volume induced local expansion and more accessible contact surface area of the nonoverlapping polymer. However, with increasing degree of polymerization this ordering *reverses* and persists in the $N \to \infty$ limit. This behavior may be a result of our tendency to overestimate the effective packing fraction of ideal chains (and hence overestimate $g(\sigma^+)$). It is conceivable that $g(\sigma^+)$ approaches a common value for all the models as $N \to \infty$.

A general feature of Figure 10 is that at high densities and large $N$ the local density of chain segments of different

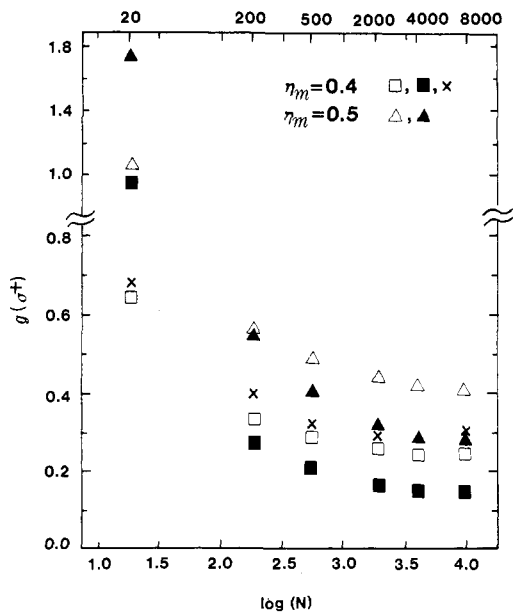


**Figure 10.** Contact value of the intermolecular radial distribution function plotted versus the logarithm of $N$. Note the break in the vertical scale and that the corresponding values of $N$ are listed along the top horizontal axis. Results are presented for the ideal freely jointed chain (open triangles and squares) and nonoverlapping freely jointed chain (solid triangles and squares) at two values of the monomer packing fraction. Results for the Gaussian chain are also shown (crosses) at the lower packing fraction.

polymers around a monomer on a tagged chain is severely reduced from the bulk value. An important question is whether this is realistic or a large $N$ artifact of the RISM theory. This issue cannot be resolved by appealing to computer simulations of high density and molecular weight off-lattice chains since they do not exist. However, several very recent *lattice* simulations do bear on this question. Kolinski, Skolnick, and Yaris[45] have calculated via Monte Carlo simulation the local intermolecular pair correlation function for athermal chains of 216 monomers at a liquidlike packing fraction of 50% on a diamond lattice. A contact value of $\simeq 0.11$ was found and corresponds to a reduction of bulk density by a factor of $0.5/0.11 \cong 4.5$. In order to crudely compare this result with our continuous space calculations it is necessary to divide the liquid packing fraction by its maximum close-packed value, which we take to be $2^{-1/2}$. Therefore, our $\eta_M = 0.4$ continuum calculation corresponds to a lattice $\phi \approx 0.56$, and for $N = 200$ we found $g(\sigma^+) \simeq 0.29$, which implies a reduction of bulk density by a factor of ≈3.5. Despite the crudity of this comparison, it does lend support to the qualitative accuracy of our RISM theory for moderately long chains and the phenomenon of significant reduction of local density by high polymer screening effects.

The situation for true high polymers is less clear. Our calculations predict a significant continuing decrease of the contact value beyond $N \approx 200$. We suspect this behavior is qualitatively correct for the highly flexible *ideal* models studied, but that such a large $N$ dependence will probably *not* survive a fully self-consistent treatment of intramolecular and intermolecular correlations. The reasoning behind our latter statement is the following. Ideal models assume that long-range intramolecular repulsions are perfectly "screened", or cancelled, on *all* length scales by the solvent (other polymer molecules) induced attractive interactions. Such models ignore repulsion-induced local chain expansion, which surely occurs especially for highly flexible polymers. The simple scheme for addressing this point presented in section III.C is only a

zero-order, *non*-self-consistent, approach. The crucial question is whether a more complete theory would yield a reduction of screening on short length scales that is strongly molecular weight dependent. In terms of the potential of mean force of eq 14, the long-range intramolecular repulsion is obviously $N$ independent, but the medium-induced attraction, $\Delta\mu$, is not. The latter feature follows from adapting the theory of Chandler et al.[33,34] to neat polymer melts, whence once can show[25] that the strength (in an integrated sense) of the medium-induced attraction is *inversely* proportional to the isothermal compressibility of the polymer melt. Physically, this reflects the fact that it costs less solvation free energy to insert a polymer molecule into a polymeric liquid if the static density fluctuations of the melt are larger, which is indeed the case for melts composed of flexible, ideal chains (see the following paper[12]). Consequently, a substantial weakening of $\Delta\mu$ with increasing molecular weight implies a less efficient *local* screening of the intramolecular excluded volume interactions. Hence, one is lead to the expectation that self-consistency corrections will increase (strongly for highly flexible polymers) with degree of polymerization, resulting in an enhancement of local chain expansion and a corresponding reduction in the $N$ dependence of the contact value. In the context of this more general self-consistent formalism, our present calculations utilizing an ideal (or nearly so) description represent the zeroth-order, or first iterative, results in a fully self-consistent scheme.

The relative packing fraction dependence of the contact value of *nonoverlapping* freely jointed chains in the dense regime is plotted in Figure 11 for several values of $N$. In contrast to the strong dependence of the *magnitude* of $g(\sigma^+)$ on $N$, the results in Figure 11 show that the *density dependence* is much less sensitive. In particular, for $N \geq 2000$ the density dependence is identical within the resolution of the figure. Another interesting trend is that the density dependence increases on going from the atomic hard-sphere limit to $N = 20$ but then reverses as the high polymer regime is entered. On the other hand, we have found that for the *ideal* freely jointed chain the density dependence of $g(\sigma^+)$ is a monotonically increasing function of $N$. These results suggest the presence of competing effects, which may involve local, small flexible molecule, liquidlike packing considerations versus correlations induced by long-range chain connectivity and self-screening in the high polymer limit. In any case, the atomic liquid displays the weakest density dependence, presumably due to the rigorous presence of only one length scale.

Finally, the asymptotic ($N \to \infty$) limiting behavior of the density dependence of $g(\sigma^+)$ is presented in Figure 12 for the three different chain models. In all three cases the density dependence is stronger than that for the atomic fluid (either Percus–Yevick[14] or the "exact" Carnahan–Starling[14]). However, for the flexible high polymers there appears to be a remarkable insensitivity to the detailed intramolecular structure. Indeed, within our ability to calculate the effective packing fraction for ideal models, the three polymer systems in Figure 12 are virtually equivalent. This surprising result implies there exists a degree of universality at large $N$ in regards to the density-induced changes in the contact value, even though the absolute magnitude of $g(\sigma^+)$ may exhibit system specificity.

## V. Summary and Conclusions

The goals of the present paper have been 2-fold. First, a generalization of our previous work on Gaussian polymer models has been pursued. In particular, the general problem of intramolecular structure has been discussed in detail with three distinct issues being considered. (1) The treatment of ideal intramolecular models beyond the Gaussian case within the RISM integral equation formalism was considered. (2) The problem of unphysical intramolecular nonbonded monomer overlap was studied. A computational scheme to approximately quantify such overlap was developed and numerically implemented. More importantly, a general procedure for rigorously removing such overlaps was developed. The resulting scheme was motivated by both general and specific screening arguments and has the virtue of retaining the basic mathematical simplicity of ideal descriptions. Quantitative implementation was carried out for the freely jointed chain, and possible experimental implications were pointed out. (3) The general problem of a self-consistent determination of the intramolecular and intermolecular correlations was discussed qualitatively, and a statistical mechanical formalism[33] to address such issues outlined.

Our second goal was to numerically study in detail for simple athermal polymer models the intermolecular radial distribution function. The sensitivity to intramolecular structure and the trends associated with variable density and degree of polymerization were elucidated. The nature of significant, system-specific, local screening was quantified, and, as far as possible, the accuracy of RISM for the local structure of relatively short chains was demonstrated. A particularly interesting finding was the sensitivity of the magnitude of $g(\sigma^+)$ to intramolecular flexibility, packing fraction, and degree of polymerization and the slow convergence to the asymptotic $N \to \infty$ values. On the other hand, the *relative* density dependence of several properties was remarkably insensitive to flexible polymer configurational statistics in the asymptotic regime.

## Appendix

The fractional overlap volume, $\epsilon_N$, can be straightforwardly determined within the superposition approximation by employing the well-known formula for the overlap volume of two spheres and $\omega_{\alpha\gamma}(r)$ for a Gaussian chain and ring and a freely jointed chain. With omission of the algebraic details, the Gaussian polymer results are

$$\epsilon_N = \frac{2}{\pi^{1/2}} \frac{1}{N} \sum_{\alpha,\gamma=1}^{N} \left[ \gamma(1.5,b_{\alpha\gamma}) - \frac{3}{2} b_{\alpha\gamma}^{-1/2} \gamma(2,b_{\alpha\gamma}) + \frac{1}{2} b_{\alpha\gamma}^{-3/2} \gamma(3,b_{\alpha\gamma}) \right] \quad \text{(A1)}$$

where $\gamma(x,y)$ is the incomplete gamma function[37] and $b_{\alpha\gamma} \equiv 3/2\mu_{\alpha\gamma}$, with

$$\mu_{\alpha\gamma} \equiv |\alpha - \gamma| \qquad \text{(chain)}$$

$$\mu_{\alpha\gamma} \equiv |\alpha - \gamma|(1 - (1/N)|\alpha - \gamma|) \qquad \text{(ring)} \quad \text{(A2)}$$

Employing Fourier transform methods yields the following result for the freely jointed chain:

$$\epsilon_N = (2/\pi N) \int_0^\infty \mathrm{d}K \, R_N(K) \, G(K) \quad \text{(A3)}$$

where

$$R_N(K) \equiv N(K/2)f(1 - f^{N-1})(1 - f)^{-1} - (K/2)f(1 - f)^{-2}[1 + Nf^{N-1}(f - 1) - f^N]$$

$$f \equiv \sin K/K \quad \text{(A4)}$$

and

$$G(K) \equiv I_1 - (3/2)I_2 + (1/2)I_4$$

$$I_n \equiv \int_0^1 \mathrm{d}x \, x^n \sin(Kx) \quad \text{(A5)}$$

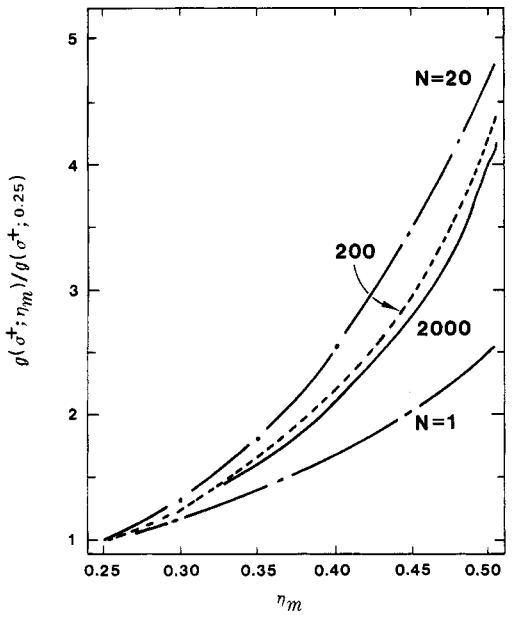


**Figure 11.** Contact value of the intermolecular radial distribution function of the nonoverlapping freely jointed chain as a function of monomer packing fraction plotted relative to its value at $\eta_M = 0.25$. Three degrees of polymerization are shown along with the Percus–Yevick hard-sphere result.

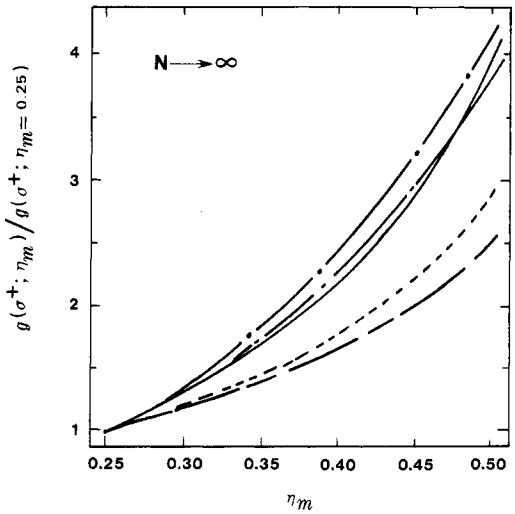


**Figure 12.** Same as Figure 11 but for different intramolecular models and in the asymptotic $N$ limit. Results for the Gaussian chain (dash-dot curve, $N = 16000$), ideal freely jointed chain (long dash, $N = 8000$), and nonoverlapping freely jointed chain (solid, $N = 4000$). In all cases the results do not change on the scale of the graph for $N$ values larger than those quoted above. The Percus–Yevick (long dash–short dash curve) and Carnahan–Starling (short-dash) hard-sphere ($N = 1$) results are also shown for comparison.

where $I_n$ can be determined in closed form.[37]

## References and Notes


(1) Schweizer, K. S.; Curro, J. G. *Phys. Rev. Lett.* **1987**, *58*, 246.
(2) Curro, J. G.; Schweizer, K. S. *Macromolecules* **1987**, *20*, 1928.
(3) Curro, J. G.; Schweizer, K. S. *J. Chem. Phys.* **1987**, *87*, 1842.
(4) Chandler, D.; Andersen, H. C. *J. Chem. Phys.* **1972**, *57*, 1930.
(5) Chandler, D. In *Studies in Statistical Mechanics VIII*; Montroll, E. W., Lebowitz, J. L., Eds.; North-Holland: Amsterdam, 1982; p 275, and references cited therein.
(6) deGennes, P.-G. *Scaling Concepts in Polymer Physics*; Cornell University: Ithaca, NY, 1979.
(7) Flory, P. J. *J. Chem. Phys.* **1949**, *17*, 203.
(8) Ballard, D. G.; Schelten, J.; Wignall, G. D. *Eur. Polym. J.* **1973**, *9*, 965. Cotton, J. P.; Decker, D.; Benoit, H.; Farnoux, B.; Higgins, J.; Jannik, G.; Ober, R.; Picot, C.; des Cloizeaux, J. *Macromolecules* **1974**, *7*, 863.
(9) Sariban, A.; Binder, K. *J. Chem. Phys.* **1987**, *86*, 5859. Sariban, A.; Binder, K.; Heerman, D. W. *Phys. Rev. B: Conds. Matter* **1987**, *35*, 6873. Cifra, P.; Karasz, F. E.; MacKnight, W. J. *Polym. Commun.* **1987**, *28*, 180.
(10) (a) Vacetello, M.; Avitabile, G.; Corradini, P.; Tuzi, A. *J. Chem. Phys.* **1980**, *73*, 543. (b) Weber, T. A.; Helfand, E. *J. Chem. Phys.* **1979**, *71*, 4760.
(11) Schweizer, K. S.; Curro, J. G. *J. Chem. Phys.*, in press.
(12) Schweizer, K. S.; Curro, J. G. *Macromolecules*, following paper in this issue.
(13) Rossky, P. J. *Annu. Rev. Phys. Chem.* **1985**, *36*, 321.
(14) Hansen, J. P.; McDonald, I. R. *Theory of Simple Liquids*; Academic: London, 1976.
(15) Gray, C. G.; Gubbins, K. E. *Theory of Molecular Fluids*; Clarendon: Oxford, 1984.
(16) Similar equations have been proposed recently in different physical contexts by Chandler et al. (see ref 33). Malescio, G.; Parrinello, M. *Phys. Rev. A* **1987**, *35*, 897. Hirata, F.; Levy, R. M. *Chem. Phys. Lett.* **1987**, *136*, 267. The relationships between the various works have been discussed by: Chandler, D. *Chem. Phys. Lett.* **1987**, *139*, 108.
(17) Lowden, L. J.; Chandler, D. *J. Chem. Phys.* **1973**, *59*, 6587.
(18) Flory, P. J. *Statistical Mechanics of Chain Molecules*; Interscience: New York, 1969.
(19) See, for example: Curro, J. G. *J. Chem. Phys.* **1976**, *64*, 2496. Curro, J. G. *Macromolecules* **1979**, *12*, 463.
(20) Flory, P. *Pure Appl. Chem.* **1984**, *56*, 305. Flory, P. *Faraday Discuss. Chem. Soc.* **1979**, *No. 68*, 14, and references cited therein.
(21) Khalatur, P. G.; Papulov, Y. G.; Pavlov, A. S. *Mol. Phys.* **1986**, *58*, 887.
(22) Theodorou, D. N.; Suter, U. W. *Macromolecules* **1985**, *18*, 1467.
(23) Casassa, E. F. *J. Polym. Sci., Part A* **1965**, *3*, 605.
(24) Yamakawa, H. *Modern Theory of Polymer Solutions*; Harper and Row: New York, 1971.
(25) Schweizer, K. S.; Curro, J. G., to be submitted for publication.
(26) Yoon, D. Y.; Flory, P. J. *Macromolecules* **1976**, *9*, 294. Fujiwara, Y.; Flory, P. J. *Macromolecules* **1970**, *3*, 289.
(27) If the polymer cannot be represented as containing only one type of spherical monomer (e.g. isotactic polystyrene), then the number of RISM equations and associated intramolecular structure factors are increased but is still typically small in number and hence the problem remains tractable.
(28) Doi, M.; Edwards, S. F. *The Theory of Polymer Dynamics*; Clarendon: Oxford, 1986.
(29) Pratt, L. R.; Hsu, C. S.; Chandler, D. *J. Chem. Phys.* **1978**, *68*, 4202.
(30) Weber, T. A. *J. Chem. Phys.* **1979**, *70*, 4277.
(31) Kolinski, A.; Skolnick, J.; Yaris, R. *Macromolecules* **1986**, *19*, 2550, 2560.
(32) Chandler, D.; Pratt, L. R. *J. Chem. Phys.* **1976**, *65*, 2925. Pratt, L. R.; Chandler, D. *J. Chem. Phys.* **1977**, *65*, 147.
(33) Chandler, D.; Singh, Y.; Richardson, D. M. *J. Chem. Phys.* **1984**, *81*, 1975.
(34) Nichols, A. L.; Chandler, D.; Singh, Y.; Richardson, D. M. *J. Chem. Phys.* **1984**, *81*, 5109.
(35) Feynman, R. P.; Hibbs, A. R. *Quantum Mechanics and Path Integrals*; McGraw-Hill: New York, 1965.
(36) Wignall, G. D.; Bates, F. S. *Bull. Am. Phys. Soc.* **1987**, *32*, 876. Bates, F. S., private communication. Ito, H.; Russell, T. P.; Wignall, G. D. *Macromolecules* **1987**, *20*, 2213.
(37) Gradshteyn, I. S.; Ryzhik, I. M. *Table of Integrals, Series, and Products*; Academic: New York, 1980.
(38) See, for example: Stoessel, J. P.; Wolynes, P. G. *J. Chem. Phys.* **1984**, *80*, 4502.
(39) Evans, K. E. *J. Polym. Sci., Polym. Lett. Ed.* **1987**, *25*, 353, and references cited therein.
(40) Ladanyi, B. M.; Chandler, D. *J. Chem. Phys.* **1975**, *62*, 4308.
(41) Andersen, H. C. *Annu. Rev. Phys. Chem.* **1975**, *26*, 145.
(42) Vargaftik, N. B. *Tables on the Thermophysical Properties of Liquids and Gases*, 2nd ed.; Wiley: New York, 1975.
(43) Chandler, D.; Hsu, C. S.; Street, W. B. *J. Chem. Phys.* **1977**, *66*, 5231. Street, W. B.; Tildesley, D. J. *J. Chem. Phys.* **1978**, *68*, 1275. Freasier, B. C.; Jolly, D.; Bearman, R. J. *Mol. Phys.* **1976**, *32*, 1463.
(44) Dickman, R.; Hall, C. K. *J. Chem. Phys.* **1986**, *85*, 4108, and references cited therein.
(45) Kolinski, A.; Skolnick, J.; Yaris, R. *J. Chem. Phys.* **1987**, *86*, 1567.